Hypothalamus-pituitary-interrenal (HPI) axis signaling in Atlantic sturgeon (*Acipenser oxyrinchus*) and sterlet (*Acipenser ruthenus*)

Ciaran A. Shaughnessy[1*], Valorie D. Myhre[1], Daniel J. Hall[2], Stephen D. McCormick[2,3], and Robert M. Dores[1]

[1] Department of Biological Sciences, University of Denver, Denver, CO
[2] U.S. Geological Survey, Eastern Ecological Science Center, S. O. Conte Anadromous Fish Research Laboratory, Turners Falls, MA, USA
[3] Department of Biology, University of Massachusetts, Amherst, MA, USA

*Corresponding author
Address: Department of Biological Sciences, University of Denver, 2101 E Wesley Ave, Denver, CO, 80208
Email: Ciaran.Shaughnessy@DU.edu
ORCID: 0000-0003-2146-9126

RUNNING HEAD

Sturgeon HPI Axis Signaling

ABSTRACT

In vertebrates, the hypothalamic-pituitary-adrenal/interrenal (HPA/HPI) axis is a highly conserved endocrine axis that regulates glucocorticoid production via signaling by corticotropin releasing hormone (CRH) and adrenocorticotropic hormone (ACTH). Once activated by ACTH, G_s protein-coupled melanocortin 2 receptors (Mc2r) present in corticosteroidogenic cells stimulate expression of steroidogenic acute regulatory protein (Star), which initiates steroid biosynthesis. In the present study, we examined the tissue distribution of genes involved in HPI axis signaling and steroidogenesis in the Atlantic sturgeon (*Acipenser oxyrinchus*) and provided the first functional characterization of Mc2r in sturgeon. Mc2r of *A. oxyrinchus* and the sterlet sturgeon (*Acipenser ruthenus*) are co-dependent on interaction with the melanocortin receptor accessory protein 1 (Mrap1) and highly selective for human (h) ACTH over other melanocortin ligands. *A. oxyrinchus* expresses key genes involved in HPI axis signaling in a tissue-specific manner that is indicative of the presence of a complete HPI axis in sturgeon. Importantly, we co-localized *mc2r*, *mrap1*, and *star* mRNA expression to the head kidney, indicating that this is possibly a site of ACTH-mediated corticosteroidogenesis in sturgeon. Our results are discussed in the context of other studies on the HPI axis of basal bony vertebrates, which, when taken together, demonstrate a need to better resolve the evolution of HPI axis signaling in vertebrates.

KEYWORDS

evolution; stress; endocrinology; fish

INTRODUCTION

The hypothalamic-pituitary-adrenal/interrenal (HPA/HPI) axis is an essential and highly conserved endocrine axis among vertebrates. The adrenal gland of most tetrapods is homologous to the interrenal tissue associated with the kidney of amphibians and fishes. The HPA/HPI axis controls glucocorticoid production and homeostasis, which mediate many key physiological functions, including metabolism, immune function, ion and water balance, and behavior (Cannon, 1929; Wendelaar Bonga, 1997). In the HPA/HPI axis of bony vertebrates, corticotropin releasing hormone (CRH) is secreted by the hypothalamus resulting in the release of the proopiomelanocortin (POMC)-derived adrenocorticotropin hormone (ACTH) by the pituitary (Wendelaar Bonga, 1997). Once in circulation, ACTH binds to the melanocortin 2 receptor (Mc2r), a G_s protein-coupled receptor which requires chaperoning by a melanocortin receptor accessory protein (Mrap1), in the glucocorticoid-producing cells of the adrenal/interrenal. Once activated by ACTH, Mc2r stimulates intracellular cAMP production, resulting in the transcriptional upregulation of the steroidogenic acute regulatory protein (Star) (Abdel-Malek, 2001), which is the rate-limiting step that initiates the biosynthesis and subsequent release of corticosteroids .

As the ACTH receptor, Mc2r occupies a critical step in the HPA/HPI axis, translating a systemic signal from the brain to the cellular process of glucocorticoid production. Two important features of Mc2r function are common to all bony vertebrates that have been examined to date: (i) Mc2r is selective for human ACTH (hereafter referred to as hACTH or simply as ACTH when discussing transactivation studies) over other melanocortin peptides, such as melanocyte stimulating hormone (MSH), and (ii) Mc2r requires chaperoning with Mrap1 for membrane trafficking and activation by ACTH (Dores and Chapa, 2021). However, these functional qualities of Mc2r in bony vertebrates appear to be derived (see Dores and Chapa (2021) for a complete review). In elasmobranchs, Mc2r is not as highly selective for ACTH over α-MSH as the Mc2r of the later bony vertebrates, and although Mrap1 enhances the trafficking of Mc2r, it does not appear to be required for activation of elasmobranch Mc2r (Dores et al., 2018; Hoglin et al., 2022; Takahashi et al., 2016). In the holocephalan (*Callorhincus milli*),

Mc2r lacks selectivity for ACTH over α-MSH and Mrap1 does not affect Mc2r activation or trafficking (Barney et al., 2019).

Given the critical functional differences between the Mc2rs of cartilaginous fishes and bony vertebrates, studies on Mc2r function in basal bony vertebrates, such as the chondrosteans, holosteans, and lobe-finned fishes, are needed to better understand the evolution of ACTH selectivity and Mrap1 dependence exhibited by Mc2r in more derived bony fishes. To this end, recent work in our laboratory has investigated Mc2r function in basal representatives from the ray-finned fishes (class Actinopterygii) side of the bony vertebrate phylogeny. Our recent studies have included functional studies on Mc2r from the only extant member in the most basal actinopterygian subclass Cladistia, the Senegal bichir (*Polypterus senegalus*) (Shaughnessy et al., 2022), a member of the basal subclass Chondrostei, the paddlefish (*Polyodon spathula*) (Dores et al., 2022), and two members of the basal neopterygian subclass Holostei, the spotted gar (*Lepisosteus oculatus*) (Wolverton et al., 2019; Wong and Dores, 2022) and the bowfin (*Amia calva*) (Dores et al., 2022; Shaughnessy et al., 2022). Together, these studies have revealed that even the most basal actinopterygians possess Mc2r which exhibit strict selectivity for ACTH over α-MSH and require co-expression of Mrap1 for membrane-trafficking and activation, functional qualities of Mc2r that are conserved across all bony vertebrates. Thus, it remains unresolved whether ACTH selectivity and Mrap1 dependence for activation were an innovation in the Mc2r of bony fishes, or ancestral traits that were lost in the cartilaginous fishes.

In addition to understanding evolutionary shifts in Mc2r function, in order to resolve the evolutionary origins of HPA/HPI axis signaling, it is equally important to understand how anatomical and molecular components of HPI axis signaling are arranged and expressed in basal vertebrates and how their arrangement and expression has changed on a macroevolutionary timescale. Numerous studies on more derived bony fishes and tetrapods have established that adrenal/interrenal-originating cortisol (and in some cases, corticosterone) is the primary glucocorticoid produced by the neuroendocrine signaling of a derived HPA/HPI axis as described above (see review by Bouyoucos et al., 2021). However, most of what we know regarding the HPI axis of bony fishes is supported only by studies in the neopterygian fishes, and relatively

little is known about the HPI axis of basal bony fishes and cartilaginous fishes. For instance, many studies in sturgeons have identified cortisol as being a stress-induced circulating corticosteroid, but the site of cortisol production and its regulation by an HPI axis have not been adequately investigated. To our knowledge, no studies have investigated the HPI axis in the bichir. In cartilaginous fishes, the novel corticosteroid 1α-hydroxycorticosterone (1α-OH-B) appears to be the predominant corticosteroid (Anderson, 2012), but the site of 1α-OH-B production and whether it is regulated by ACTH signaling from a hypothalamus-pituitary axis has not been directly investigated. In the more basal jawless vertebrates, including the lampreys, 11-deoxycortisol is the circulating corticosteroid in response to stress (Close et al., 2010; Shaughnessy and McCormick, 2021) but the site of 11-deoxycortisol production and its regulation by ACTH signaling from a hypothalamus-pituitary axis is not well-understood.

In the present study, we utilized newly available genomic resources and cell-based assays to identify, express, and study the function of Mc2r from two sturgeon species, the Atlantic sturgeon (*Acipenser oxyrinchus*) and the sterlet (*Acipenser ruthenus*). We examined the Mc2rs of *A. oxyrinchus* and *A. ruthenus* for their ligand specificity and co-dependence on interaction with Mrap1. We further investigated the HPI axis of *A. oxyrinchus* by examining the anatomical arrangement and molecular expression of critical genes known to be involved in the neuroendocrine signaling pathway of a derived HPI axis. We sought to test the hypotheses that sturgeons, as representatives of a basal subclass of Actinopterygii, possess an Mc2r that is selective for ACTH and co-dependent on interaction with Mrap1, and express genes in a tissue-specific manner that is indicative of the presence of a complete HPI axis.

METHODS

2.1 Sequence Discovery and Analyses

Available genome assemblies for *A. oxyrinchus* (ASM1318447v1) and *A. ruthenus* (ASM1064508v1) were accessed from the National Center for Biotechnology Information (NCBI) GenBank. Using the BLAST (Basic Local Alignment Search Tool) from NCBI, we surveyed the *A. oxyrinchus* (ao) and *A. ruthenus* (ar) genomes for nucleotide sequences corresponding to *mc2r*, *mrap1*, and *mrap2*. Additionally, we

further surveyed the *A. oxyrinchus* genome for nucleotide sequences corresponding to *crh*, *crhr*, *pomc*, and *star*. The Translate tool from ExPASy (https://www.expasy.org) was used to deduce amino acid sequences of aoMc2r, aoMrap1, aoMrap2, and arMc2r. The TMHMM tool from the DTU Bioinformatics Server (https://www.bioinformatics.dtu.dk) was used to predict hypothetical membrane topology. A selection of gnathostome Mc2r and Mrap amino acid sequences obtained from NCBI GenBank were used in multiple sequence alignment and phylogenetic analyses. Multiple sequence alignments were performed using the Clustal Omega multiple sequence alignment tool available from the European Bioinformatics Institute (https://www.ebi.ac.uk/tools/msa/) and arranged using BioEdit software (Hall, 1999), with modifications to ensure the alignment of functional motifs following previously described methods (Dores et al., 1996). Phylogenetic analyses were performed using MEGA10 software (Kumar et al., 2008) and implemented the neighbor-joining method (1,000 bootstrap replicates).

Accession numbers for the amino acid sequences from species other than sturgeons used in our analyses were: elephant shark Mc2r (*Callorhinchus milii*; FAA00704), whale shark Mc2r (*Rhincodon typus*; XP_020380838), stingray Mc2r (*Hemitrygon akajei*; BAU98231), bichir Mc2r (*Polypterus senegalus*; XM_039738597), gar Mc2r (*Lepisosteus oculatus*; XP_006636159), rainbow trout Mc2r (*Oncorhynchus mykiss*; ABV23494), carp Mc2r (*Cyprinus carpio*; CAE53845), zebrafish Mc2r (*Danio rerio*; AAO24743), lungfish Mc2r (*Protopterus annectens*; XP_043923917), frog Mc2r (*Xenopus tropicalis*; XP_002936118), chicken MC2R (*Gallus gallus*; AGR42637), mouse MC2R (*Mus musculus*; NP_001288301), human MC2R (*Homo sapiens*; NP_001278840), whale shark Mrap1 (XP_020375601), whale shark Mrap2 (XP_020377388), gar Mrap1 (ENSLOCP00000011199), gar Mrap2 (XP_015205283), rainbow trout Mrap1 (NP_001233276), rainbow trout Mrap2 (NP_001233282), chicken MRAP1 (XR_001470382), chicken MRAP2 (XP_046770071), mouse MRAP1 (NP_084120), mouse MRAP2 (NP_001346884), human MRAP1 (AAH62721), and human MRAP2 (AIC52816). Sequences for bowfin (*Amia calva*) Mc2r, Mrap1, and Mrap2 were obtained as a gift from the authors of the recently published bowfin genome (Thompson et al., 2021).

2.2 Cell Culture, Transfection, and Reporter Gene Assay

Sturgeon Mc2r function was analyzed using a cAMP-responsive luciferase reporter gene assay carried out in Chinese hamster ovary (CHO) cells, as previously described (Liang et al., 2011; Reinick et al., 2012). CHO cells are commonly used for Mc2r functional studies because they do not endogenously express Mc2r or Mrap1 proteins (Noon et al., 2002; Reinick et al., 2012; Sebag and Hinkle, 2007).

Transfections were performed using commercially obtained *mc2r* and *mrap1* cDNA constructs as inserts on a pcDNA3.1+ expression vector (GenScript; Piscataway, NJ). During transfection, plasmid vectors (2 µg per 1×10^5 cells) were inserted into CHO cells (ATCC; Manassas, VA) using a Solution T kit for the Amaxa Nucleofector 2b system (Lonza; Portsmouth, NH). Depending on the experiment, *mc2r* cDNA constructs were transfected with or without co-transfection of cDNA constructs of various gnathostome *mrap1*s. Regardless of the experiment, all CHO cells were also co-transfected with a cAMP reporter construct, a *luciferase* gene promoted by a cAMP-responsive element (CRE-Luciferase) that was transfected at 2.5 µg per 1×10^5 cells (Chepurny and Holz, 2007). Thus, a maximum total of 3 simultaneous transfections were performed for any given experiment. Transfected CHO cells were seeded at a density of 3×10^5 cells cm^{-2} into opaque 96-well cell culture plates (Cat. No. 3912; Corning Life Sciences; Manassas, VA). Cells were cultured at 37 °C under 5% CO_2 for 48 h in a DMEM/F12 media (Cat. No. 11320-033; Gibco, UK) supplemented with 10% fetal calf serum and 1% penicillin-streptomycin. After 48 h culture post-transfection, the culture media was removed, and cells were stimulated with either human ACTH(1–24) or α-MSH (New England Peptide, Gardner, MA) in serum-free DMEM/F12 media, then placed back into incubation for an additional 4 h to allow any Mc2r-mediated cAMP production to occur. Concentrations of ACTH and α-MSH ranged from 10^{-6}–10^{-12} M. After stimulation, media was removed and replaced with a luciferase substrate (BrightGLO; Promega; Madison, WI), and the luminescence generated after 5 min was measured spectrophotometrically by a BioTek Synergy HT microplate reader using Gen5 software (Agilent Technologies; Santa Clara, CA). Luminescence values (measured as relative light units) of an unstimulated (0 M ligand) control for each unique

transfection were subtracted from all other luminescence readings, as a background correction step.

2.3 Live Animal Care and Tissue Sampling

Handling and care of *A. oxyrinchus* followed procedures approved by the Internal Animal Care and Use Committees at the University of Massachusetts (Protocol No. 2016–0009) and U.S. Geological Survey (Protocol No. C0907). Juvenile *A. oxyrinchus* were obtained 14 d post-hatch from Bears Bluff National Fish Hatchery (USFWS, Wadmalaw Island, SC, USA) and reared at the Conte Anadromous Fish Research Laboratory (USGS, Turners Falls, MA, USA). Sturgeon were held in 1.5 m diameter tanks supplied with 4 L min^{-1} of dechlorinated municipal water under natural photoperiod and ambient temperature, and fed a progression of diets as they grew: first a diet of only live brine shrimp, then a diet containing a mixture of bloodworms and a fine commercial pellet (Otohime, Reed Mariculture, Inc., USA), then a diet of only a standard commercial pellet (Bio-Oregon, USA).

Tissue samples were collected from *A. oxyrinchus* (n = 3) that were 1 year old (22.7 ± 3.3 cm total length; 39.9 ± 16.4 g mass). During sampling, sturgeon were euthanized using a lethal dose of MS-222 (200 mg L^{-1} buffered using $NaHCO_3$, pH 7.4), measured for body length and mass, then sampled for tissues. Tissues samples included: brain (all regions except pituitary), pituitary, gill, heart, liver, head kidney (anterior most region of kidney), kidney, intestine (anterior region), spiral valve, white muscle, and gas bladder. Tissues were immediately frozen and stored at -80 °C for later RNA extraction.

2.4 Gene Expression Analyses

Following the manufacturer-supplied protocol, total RNA was isolated from frozen tissue using a TRIzol method (Molecular Research Center Inc.). RNA was quantified and analyzed for purity using a Nanodrop 2000 spectrophotometer (Thermo Scientific Inc.). Only high-purity samples (A260/A280 > 1.8) were used for further analyses. First-strand cDNA synthesis was performed using a high-capacity reverse transcription kit following the manufacturer-supplied protocol (Applied Biosystems Inc.). Quantitative PCR was performed using SYBRselect Master Mix (Applied Biosystems) and a QuantStudio™ 3

Real-Time PCR System (Applied Biosystems). The analyses were carried out in 10 µL reactions containing 4 ng cDNA, 150 nM forward and reverse primers, and 2X SYBRselect master mix. The reaction cycle consisted of the following protocol: 2 min at 50 °C, 2 min at 95 °C (holding and activation), 40 cycles of 15 s at 95 °C, 1 min at 60 °C, 30 s at 72 °C (cycling). After cycling, a melt curve analysis (thermal ramp from 60 to 95 °C) was performed to confirm a single product in each reaction. Relative mRNA abundance of genes of interest are presented as $2^{-\Delta CT}$ using β-actin (*actb*), glyceraldehyde-3-phosphate dehydrogenase (*gapdh*), and elongation factor 1 alpha (*ef1a*) as reference genes (modified from Pfaffl, 2001). In calculating $2^{-\Delta CT}$, the geometric mean of the C_T values of the reference genes was used as a reference value. Information for primer pairs targeting *actb, gapdh, ef1a, crh, crhr, pomca, pomcb, mrap1, mc2r, star,* and *cyp11a1* genes from *A. oxyrinchus* are provided in Table I.

2.5 Calculations and Statistical Analyses

Receptor activation dose-response curves were analyzed using non-linear regression (three-parameter polynomial; log([ligand]) vs luminescence). Values for half-maximal effective concentration (EC_{50}) and maximal response (V_{max}) were obtained from the fitted curves and compared using the extra-sum-of-squares F test ($\alpha = 0.05$). All statistics and figure preparation were performed using Prism 9 software (GraphPad Inc., La Jolla, CA). All data are presented as mean ± standard error ($n = 3$).

RESULTS

3.1 *Sequence Analyses*

Within the *A. oxyrinchus* genome assembly, we identified sequences for *actb*, *crh, crhr,* two *pomc* genes (*pomca* and *pomcb*), *mc2r*, *mrap1*, and *star* (see NCBI Accession Nos. listed in **Table I**). Additionally, we identified a sequence for *mrap2* (Accession No. JABEPO010267884). Within the *A. ruthenus* genome assembly, we identified a sequence for *mc2r* (Accession No. NC_048325). The deduced amino acid sequences for *A. oxyrinchus* and *A. ruthenus* Mc2r aligned with human MC2R (**Fig. 1A**), with sequence similarities to human MC2R of 56.9% and 56.2%, respectively. The two sturgeon Mc2r sequences were 97.4% similar and formed a monophyletic clade within

the phylogeny of gnathostome Mc2r sequences (**Fig. 1B**). The *A. oxyrinchus* Mrap1 gene aligned with other gnathostome Mrap1 orthologues with notably high sequence similarity within the δ-D-Y-δ activation motif (bony vertebrates only; Dores and Chapa, 2021), the reverse topology motif, and the membrane trafficking motif (**Fig. 1C**). Likewise, the *A. oxyrinchus* Mrap2 aligned with other gnathostome Mrap2, which are notably missing an intact δ-D-Y-δ activation motif. The phylogenetic analysis of *A. oxyrinchus* Mraps placed aoMrap1 and aoMrap2 among the respective gnathostome Mrap1 and Mrap2 clades (**Fig. 1C**).

3.2 *Activation of Sturgeon Mc2r*

As we were only able to identify an Mrap1 orthologue from *A. oxyrinchus* and not *A. ruthenus*, we first sought to test and compare Mrap1 dependence and ACTH selectivity of the two sturgeon Mc2r orthologs using an identical set of heterologous gnathostome Mrap1 orthologs, from bowfin, chicken, and whale shark. Expression of either sturgeon Mc2rs without an Mrap1 resulted in no activation of the receptors by the ACTH ligand (**Fig. 2A-B**). Co-expression of both Mc2rs with Mrap1 resulted in substantial activation by ACTH. However only bowfin (bf) Mrap1 and chicken (ch) MRAP1 enabled the activation of sturgeon Mc2r by ACTH; co-expression with whale shark (ws) Mrap1 resulted in no activation of sturgeon Mc2r (**Fig. 2A-B**). The EC_{50} values of aoMc2r co-expressed with bfMrap1 was almost 10-fold higher than that with chMRAP1 ($F_{1,36}$ = 27.0; P < 0.001) (**Table II, Fig. 2A**). The EC_{50} values of arMc2r co-expressed with bfMrap1 and chMRAP1 were not significantly different ($F_{1,36}$ = 0.02; P = 0.877) (**Table II, Fig. 2B**).

In a subsequent experiment, we co-expressed each of the sturgeon Mc2rs with bfMrap1 and compared activation of Mc2r by ACTH and α-MSH ligands. Both sturgeon Mc2rs were activated by ACTH (**Fig. 2C-D**), replicating the approximate EC_{50} values of the previous experiment (**Table II**). No activation of aoMc2r by α-MSH was observed (**Fig. 2C**). We observed sub-saturating activation of arMc2r by α-MSH at the highest concentration ligand (10^{-6} M), indicating that arMc2r has at least a 100,000-fold higher sensitivity for ACTH over α-MSH, which was a highly significant difference ($F_{1,36}$ = 21.3; P < 0.001) (**Fig. 2D**).

With a characterization of the sturgeon Mc2rs co-expressed with heterologous Mrap1s as a baseline, we sought to test the action of a sturgeon-specific Mrap1 and Mrap2 (from *A. oxyrinchus*; aoMrap1 and aoMrap2, respectively) in affecting function of the sturgeon Mc2rs. As was observed in previous experiments, ACTH did not activate the sturgeon Mc2rs when they were expressed alone but did activate the sturgeon Mc2rs when they were co-expressed with aoMrap1 (**Fig. 3A-C**); aoMc2r could not be activated by ACTH when co-expressed with aoMrap2 (**Fig. 3A**). The EC_{50} values of ACTH-stimulated aoMc2r and arMc2r when co-expressed with aoMrap1 were similar to those values observed when co-expressed with bfMrap1 and chMRAP1 (**Table II**).

Both sturgeon receptors exhibited only sub-saturating activation by α-MSH at the highest concentration (**Fig. 3B-C**), a comparatively much lower potency for activating sturgeon Mc2rs than ACTH (aoMc2r: $F_{1,36} = 15.8$, $P < 0.001$; arMc2r: $F_{1,36} = 4.3$; $P < 0.019$) (**Fig. 3B-C**).

3.3 *Tissue Profiles of HPI Axis Gene Expression*

For every *A. oxyrinchus* gene-of-interest that we evaluated for mRNA transcript abundance (*crh, crhr, pomc, mc2r, mrap1,* and *star*), we were able to design homologous gene-specific primers using the available *A. oxyrinchus* genome that produced efficient, target-specific amplification (**Fig. 4A**) and allowing for the evaluation of tissue-specific expression by real-time PCR (**Fig. 4B-G**).

Expression of *crh* was highest in the brain, heart, and muscle (**Fig. 4B**), which all expressed *crh* at similarly high levels, approximately 4-fold higher than the next highest *crh*-expressing tissues. Expression of *crhr* was equally high in the brain, pituitary, and heart, which all expressed *crhr* at least 10-fold higher than the next highest *crhr*-expressing tissues (**Fig. 4C**). Two paralogs of *pomc* were identified in the *A. oxyrinchus* genome, which correspond to the two *pomc* paralogs previously identified in the white sturgeon (*Acipenser transmontanus*) (Alrubaian et al., 1999; Amemiya et al., 1997). These two *pomc* paralogs (*pomca* and *pomcb*) were nearly exclusively expressed in the pituitary, ~1,000–2,000-fold higher expression than any other tissue (**Fig. 4D-E**). Interestingly, *mc2r* was more highly expressed (~2-fold) in the liver than the head kidney, with the next highest *mc2r*-expressing tissue being the intestine and spiral valve

(**Fig. 4F**). Expression of *mrap1* was more similarly expressed across tissues than any other gene investigated here, and was highest expressed in the liver, head kidney, intestine, and spiral valve (**Fig. 4G**).

We were unable to identify any tissue or structure in *A. oxyrinchus* that resembled the *star*-expressing yellow corpuscles that were identified in the white sturgeon (*Acipenser transmontanus*) (Kusakabe et al., 2009) (**Fig. 5A-B**). Instead, expression of *star* was nearly exclusive to the head kidney, expressed at levels at least 150-fold higher than any other tissue (**Fig. 5C,D**). Expression of *cyp11a1* was also prominent in the head kidney, at ~15-fold higher than any other tissue except the gill, which also had prominent expression of *cyp11a1* mRNA **(Fig. 5C,E)**.

DISCUSSION

Our functional studies on Mc2r revealed that the sturgeon Mc2rs, like all other bony vertebrate Mc2rs studied to date, were dependent on interaction with Mrap1 and selective for ACTH over α-MSH. Although both sturgeon Mc2rs generally interacted with Mrap1 and melanocortin ligands in a similar manner, some differences between them are worth discussing. In our analysis examining ACTH activation of sturgeon Mc2r co-expressed with heterologous vertebrate Mrap1s, both aoMc2r and arMC2r were unable to be activated by ACTH when co-expressed with wsMrap1 and exhibited similar EC_{50} values as each other when co-expressed with either bfMrap1 or chMrap1. However, aoMc2r produced more luciferase activity (i.e., had a higher V_{max}) when co-expressed with bfMrap1 compared to chMRAP1, and the opposite was true for arMc2r, which produced more luciferase activity when co-expressed with chMRAP1 compared to bfMrap1 (**Fig. 2A-B**). A higher V_{max} could indicate a higher efficacy of Mrap1-mediated membrane trafficking of Mc2r, and analysis of the cell surface expression of Mc2r could help resolve this discrepancy between aoMc2r and arMc2r.

Another notable feature of the two sturgeon Mc2rs was observed in their affinity for melanocortin ligands. When the sturgeon Mc2rs were co-expressed with bfMc2r, aoMc2r demonstrated exclusive selectivity for ACTH but arMc2r was able to be activated by α-MSH at the highest concentration (**Fig. 2**) It should be noted that arMc2r activation of α-MSH was still only sub-saturating even at the highest concentration (10^{-6}

M), which is supraphysiological. A similar observation was made when the sturgeon Mc2rs were co-expressed with the sturgeon Mrap1, where some Mc2r activation by α-MSH was observed, although the action of α-MSH was still only sub-saturating and only observed at the highest, supraphysiological concentration. Likewise, the ACTH selectivity of arMc2r again appeared to be slightly less robust than that of aoMc2r (**Fig. 3**). The only other chondrostean Mc2r to be functionally examined in this way was the Mc2r of the paddlefish (*Polyodon spathula*), which was also able to be activated by α-MSH at supraphysiological concentrations of the ligand (Dores et al., 2022). Similarly, it has been previously observed that the Mc2r of the holostean, the gar (*L. osseus*), was also able to be activated by α-MSH at supraphysiological levels (Wolverton et al., 2019; Wong and Dores, 2022).

The observations that Mc2r in chondrosteans and holosteans have some affinity for α-MSH may reflect a transitional evolutionary state of the ACTH receptor. The Mc2rs of more basal vertebrates, the cartilaginous fishes, are not completely dependent on Mrap1 chaperoning and not exclusively selective for ACTH (Barney et al., 2019; Dores and Chapa, 2021; Hoglin et al., 2022). Thus, there appears to have been an important shift toward Mrap1 dependence and ACTH selectivity in Mc2r function during the emergence of bony vertebrates. It is known that Mc2r has exhibited more rapid sequence divergence compared to other Mcrs (Schiöth et al., 2005; Wong and Dores, 2022), and it is hypothesized that Mc2r has evolved to be more Mrap1 dependent and selective for ACTH (Dores et al., 2016; Dores and Chapa, 2021). In this context, it is possible that basal actinopterygian Mc2rs illustrate intermediary forms of an evolving Mc2r gene, from a receptor that is minimally or not at all selective for ACTH (in the cartilaginous fishes) to one that is selective for ACTH over α-MSH at even supraphysiological concentrations (in the more derived bony vertebrates). More studies on the structure and function of the Mc2rs of basal bony vertebrates (especially from the sarcopterygian side of the bony vertebrate monophyly) and additional cartilaginous fishes are needed to further elucidate the timing of acquisition of Mrap1 dependence and ACTH selectivity during vertebrate evolution.

Generally, *crh* and *crhr* are known to be abundantly expressed in the brain and pituitary, respectively, with relatively limited expression in other tissues (Dautzenberg et

al., 2001). However, in Darby's sturgeon (*Acipenser darbyanus*), *crh* is widely expressed across many tissues (Qi et al., 2019). In the present study, we too observed *crh* expression in many tissues of *A. oxyrinchus*, albeit with much greater differences in *crh* expression among tissues—the brain (excluding the pituitary), heart, and muscle had much higher *crh* expression than other tissues. Although the role of *crh* in the heart and muscle in *A. oxyrinchus* is unclear, it does reflect similar expression of CRH receptors in the heart and muscle in tetrapods (Dautzenberg et al., 2001). CRH and urocortins have known cardioprotective roles in mammals by, among other mechanisms, increasing vasodilation and preventing apoptosis (Davidson et al., 2009). Cardioprotective effects of CRH and urocortins have also been described in zebrafish (Williams et al., 2017). Two receptors of CRH (*crhr1* and *crhr2*) have been identified in *A. darbyanus,* with *crhr1* being expressed relatively equally across all tissues examined and *crhr2* being more highly expressed in the stomach (and to a lesser extent the gills) than any other tissue (Qi et al., 2019). In *A. oxyrinchus*, we could only identify a single *crhr* sequence and found it to be highly expressed in the pituitary and brain, supporting our hypothesis of the presence of a CRH-mediated hypothalamus-pituitary connection regulating ACTH production in an HPI axis in sturgeon. Interestingly, in addition to the brain and pituitary, the heart of *A. oxyrinchus* also highly expressed *crhr*. Together, the high expression of *crh* and *crhr* in the heart of *A. oxyrinchus* warrant further investigation into the peripheral action of CRH in sturgeon. Unfortunately, the tissue distribution presented for Darby's sturgeon did not include heart or muscle (Qi et al., 2019), so, at present, comparisons cannot be made between the two species of sturgeons regarding *crh* and *crhr* expression in these tissues.

Although only a single *pomc* orthologue has been identified in both spotted gar (*Lepisosteus osseus*) (Dores et al., 1997) and *P. senegalus* (Bagrosky et al., 2003), two *pomc* orthologues, *pomca* (Amemiya et al., 1997) and *pomcb* (Alrubaian et al., 1999), have been found in the pituitary of white sturgeon (*Acipenser transmontanus*). In the present study, we also identified two *pomc* genes (*pomca* and *pomcb*) in the genome of *A. oxyrinchus*. As expected, these two genes were exclusively expressed in the pituitary. Multiple *pomc* orthologues have also been identified in various teleosts (Arends et al., 1998; Cardoso et al., 2011; Okuta et al., 1996; Valen et al., 2011;

Winberg and Lepage, 1998; Wunderink et al., 2012). In some species, it has been observed that only a single *pomc* orthologue exhibits stress-responsiveness (Leder and Silverstein, 2006; Wunderink et al., 2012), where as in other species, both *pomc* orthologues have been shown to be stress-responsive (Valen et al., 2011; Winberg and Lepage, 1998). In *A. transmontanus*, canulation-administered hACTH(1-24) increased circulating cortisol concentrations within 1 h (Belanger et al., 2001). However, potential differences in the physiological role(s) of each *pomc* orthologues in sturgeon is yet to be explored. Future studies should examine whether *pomca*, *pomcb*, or both are involved in regulating constitutive or stress-responsive corticosteroidogenesis in sturgeon.

Mc2r is classically known to be the receptor that receives an ACTH signal and initiates adrenocorticosteroidogenesis. Thus, in the derived bony vertebrates, Mc2r expression is known to be highly specific to the corticosteroidogenic cells of the adrenal/interrenal tissue (Abdel-Malek, 2001). Tissue-specific expression of *mc2r* has been far less studied in basal bony vertebrates. In the gar, *L. osseus*, *mc2r* expression was highly abundant in the anterior-most region of the kidney (Wong and Dores, 2022). Interestingly, *mc2r* expression was also observed in the gills of *L. osseus* (Wong and Dores, 2022), though its physiological role in the gills was not examined. In the present study in *A. oxyrinchus*, *mc2r* expression was highest in the liver, then the head kidney, then the intestine and spiral valve. High expression of *mc2r* in the liver is interesting and has been observed at least once before, in sea bass (*Dicentrarchus labrax*) (Agulleiro et al., 2013) where it was shown that hACTH(1-24) could modulate hepatic lipolysis, presumably mediated by hepatic Mc2r. It is possible that, in addition to stimulating Mc2r-mediated steroidogenesis in the adrenal/interrenal, some actinopterygians have evolved to utilize ACTH to regulate phosphokinase A (PKA)-mediated hepatic glucose release by activating Mc2r in the liver. In addition to high expression of *mc2r* in the liver, high expression of *mc2r* in the head kidney of *A. oxyrinchus* supports the hypothesis that a pituitary-derived ACTH signal targets interrenal steroidogenic tissue (see discussion on *star* expression below) to form a complete HPI axis in sturgeon.

Finally, we evaluated the tissue-specific expression of *star* and *cyp11a1* to identify corticosteroidogenic tissue in *A. oxyrinchus*. Previous studies have sought to identify steroidogenic tissue in sturgeons. In *A. oxyrinchus*, steroidogenic activity and

adrenocortical cells have been identified in novel structures, referred to as yellow corpuscles, located along the kidney (Idler and O'Halloran, 1970; Idler and Sangalang, 1970). These yellow corpuscles have also been identified in two other species of sturgeon, the lake sturgeon (*A. fulvescens*) (Youson and Butler, 1976) and the white sturgeon (*A. transmontanus*) (Kusakabe et al., 2009). In *A. transmontanus*, yellow corpuscles were further demonstrated to have relatively high abundance of *star* expression (Kusakabe et al., 2009). Adrenocortical tissue has also been identified in yellow corpuscles in other basal bony fish groups, including the cladistians reedfish (*Calamoichthys calabaricus*) (Youson et al., 1988), Palmas bichir (Polypterus palmas) (Youson and Butler, 1985), and the holostean bowfin (*A. calva*) (Butler and Youson, 1986; De Smet, 1962). However, in another holostean, the spotted gar (*L. osseus*), for which *star* and *mc2r* expression were assessed across longitudinal regions of the kidney, and it was observed that the most anterior region of the kidney had the highest expression of both *star* and *mc2r* (Wong and Dores, 2022), and no mention of yellow corpuscles was made.

It is perplexing why we could not identify yellow corpuscles along the kidney tissue in our Atlantic sturgeon specimens (**Fig. 5A-B**). One possible explanation is that the appearance of adrenocorticortical yellow corpuscles in the sturgeon kidney is developmentally determined. Previous studies identifying these yellow bodies in sturgeons have used fish that were at least one year older and up to five times larger than the fish used in our study. It is possible that yellow corpuscles appear in the kidney tissue later in development than the age/size of our specimens. A related possible explanation is that adrenocortical structures representing precursors to the mature yellow corpuscles were indeed present in the head kidney of *A. oxyrinchus* but were too small or undeveloped for us to identify.

The present study is the first to describe the tissue-specific expression of *star* in *A. oxyrinchus* and *cyp11a1* in any sturgeon species. In *A. transmontanus*, *star* mRNA was approximately 67 times more abundant in the yellow corpuscles than the posterior kidney (Kusakabe et al., 2009). In *A. oxyrinchus* in the present study, *star* mRNA was over 200 times more abundant in the head kidney than the posterior kidney (see **Fig. 5**). In the Siberian sturgeon (*Acipenser baerii*), highest *star* expression was observed in

kidney tissue among a profile of several different tissues (Berbejillo et al., 2012), although it was unclear whether the kidney sample included the head kidney and whether the presence of yellow corpuscles was investigated. As for *cyp11a1*, like for *star*, we observed highest expression of *cyp11a1* in the head kidney of *A. oxyrinchus*. However, unlike for *star*, we also detected relatively high expression of *cyp11a1* in another tissue, the gills. It is unclear what the role of Cyp11a1 in the gills might be, warranting further investigation.

Our work demonstrates the need to reconsider the possibility that chondrosteans, in addition to having corticosteroidogenic activity in yellow corpuscles, have corticosteroidogenic activity in interrenal tissue of the head kidney similar to the interrenal tissue of all other later-evolved fishes, and that the sturgeon interrenal tissue is involved in a stress-responsive HPI axis. Only Kusakabe et al. (2009) have investigated the stress-responsiveness of corticosteroidogenesis in the yellow corpuscles of sturgeon, and it was observed that acute stress did not affect *star* expression in the yellow corpuscles of *A. transmontanus* (Kusakabe et al., 2009). Additional studies on stress-responsive steroidogenesis in chondrostean fishes are needed to better understand the localization and regulation of Star and steroidogenic enzymes during stimulation of the HPI axis.

In conclusion, in the present study we examined the function of sturgeon ACTH receptors (Mc2rs) and the tissue distribution of mRNA transcript levels of *mc2r* and other genes involved in HPI axis signaling in sturgeon. We demonstrated that sturgeon Mc2r is co-dependent on Mrap1 chaperoning and highly selective for ACTH over α-MSH. The Mrap1 dependence and ACTH selectivity exhibited by sturgeon Mc2rs are reflective of the functional qualities of all other bony vertebrate Mc2rs studied to date, although the ability of sturgeon Mc2r to be activated by supraphysiological concentrations of α-MSH may reflect some vestigial functional qualities of Mc2r present in the more basal cartilaginous fishes. Additionally, we demonstrated that *A. oxyrinchus* expresses key genes in a tissue-specific manner that is consistent with the classically understood arrangement of HPI axis signaling in more derived bony vertebrates. Importantly, we co-localized *mc2r, mrap1,* and *star* expression to the head kidney, indicating that this is a possible site of ACTH-mediated steroidogenesis in sturgeon. Our

work underscores the need for further studies on basal bony vertebrates and cartilaginous fishes to better resolve the evolution of HPI axis signaling in vertebrates.

ACKNOWLEDGEMENTS

We thank A. Regish, J. Norstog, D. Ferreira-Martins, and A. Barany for their support and assistance in animal care and sampling. We thank B. McGinley for their support and assistance in receptor activation studies. We thank P.M. Hinkle for providing the cDNA construct of CRE-Luciferase.

FUNDING

This research was supported by the Long Research Endowment at the University of Denver to R.M.D., a National Science Foundation Postdoctoral Fellowship (DBI-2109626) to C.A.S., a National Science Foundation grant (IOS-1558037) to S.D.M., and a University of Denver Undergraduate Research Center Summer Fellowship to V.M.

DISCLOSURES

The authors declare that they have no known competing financial or personal interests regarding the studies presented in this manuscript. Any use of trade, firm, or product names is for descriptive purposes only and does not imply endorsement by the U.S. Government.

AUTHOR CONTRIBUTIONS

CAS: conceptualization, methodology, investigation, formal analysis, data curation, visualization, writing (original draft, editing, review of final draft), funding acquisition.
VM: conceptualization, methodology, investigation, formal analysis, data curation, visualization, writing (review of final draft).
DJH: methodology, investigation, writing (review of final draft).
SDM: investigation, writing (review of final draft), supervision, project administration, funding acquisition.
RMD: conceptualization, methodology, investigation, formal analysis, writing (editing, review of final draft), supervision, project administration, funding acquisition.

LITERATURE CITED

Abdel-Malek, Z. a, 2001. Melanocortin receptors: their functions and regulation by physiological agonists and antagonists. Cell Mol Life Sci 58, 434–441. https://doi.org/10.1007/PL00000868

Agulleiro, M.J., Sánchez, E., Leal, E., Cortés, R., Fernández-Durán, B., Guillot, R., Davis, P., Dores, R.M., Gallo-Payet, N., Cerdá-Reverter, J.M., 2013. Molecular Characterization and Functional Regulation of Melanocortin 2 Receptor (MC2R) in the Sea Bass. A Putative Role in the Adaptation to Stress. PLoS One 8. https://doi.org/10.1371/journal.pone.0065450

Alrubaian, J., Danielson, P., Fitzpatrick, M., Schreck, C., Dores, R.M., 1999. Cloning of a second proopiomelanocortin cDNA from the pituitary of the sturgeon, Acipenser transmontanus. Peptides 20, 431–436. https://doi.org/10.1016/S0196-9781(99)00021-2

Amemiya, Y., Takahashi, A., Dores, R.M., Kawauchi, H., 1997. Sturgeon proopiomelanocortin has a remnant of γ-melanotropin. Biochem Biophys Res Commun 230, 452–456. https://doi.org/10.1006/bbrc.1996.5987

Anderson, W.G., 2012. The endocrinology of 1α-hydroxycorticosterone in elasmobranch fish: a review. Comp Biochem Physiol - A Mol Integr Physiol 162, 73–80. https://doi.org/10.1016/j.cbpa.2011.08.015

Arends, R.J., Vermeer, H., Martens, G.J.M., Leunissen, J.A.M., Bonga, S.E.W., Flik, G., 1998. Cloning and expression of two proopiomelanocortin mRNAs in the common carp (Cyprinus carpio L.). Mol Cell Endocrinol 143, 23–31. https://doi.org/10.1016/S0303-7207(98)00139-7

Bagrosky, B., Lecaude, S., Danielson, P.B., Dores, R.M., 2003. Characterizing a proopiomelanocortin cDNA cloned from the brain of the Bichir, Polypterus senegalus: Evaluating phylogenetic relationships among ray-finned fish. Gen Comp Endocrinol 134, 339–346. https://doi.org/10.1016/j.ygcen.2003.09.014

Barney, E., Dores, M.R., McAvoy, D., Davis, P., Racareanu, R.C., Iki, A., Hyodo, S., Dores, R.M., 2019. Elephant shark melanocortin receptors: Novel interactions with MRAP1 and implication for the HPI axis. Gen Comp Endocrinol 272, 42–51.

https://doi.org/10.1016/j.ygcen.2018.11.009
Belanger, J.M., Son, J.H., Laugero, K.D., Moberg, G.P., Doroshov, S.I., Lankford, S.E., Cech Jr., J.J., 2001. Effects of short-term management stress and ACTH injections on plasma cortisol levels in cultured white sturgeon , Acipenser transmontanus. Aquaculture 203, 165–176.
Berbejillo, J., Martinez-Bengochea, A., Bedo, G., Brunet, F., Volff, J.N., Vizziano-Cantonnet, D., 2012. Expression and phylogeny of candidate genes for sex differentiation in a primitive fish species, the Siberian sturgeon, Acipenser baerii. Mol Reprod Dev 79, 504–516. https://doi.org/10.1002/mrd.22053
Bouyoucos, I.A., Schoen, A.N., Wahl, R., Anderson, W.G., 2021. Ancient fishes and the functional evolution of the corticosteroid stress response in vertebrates. Comp Biochem Physiol - A Mol Integr Physiol 260, 111024. https://doi.org/10.1016/j.cbpa.2021.111024
Butler, D.G., Youson, J.H., 1986. Steroidogenesis in the yellow corpuscles (Adrenocortical homolog) in a holostean fish, the bowfin, Amia calva L. Gen Comp Endocrinol 63, 45–50. https://doi.org/10.1016/0016-6480(86)90180-2
Cannon, W.B., 1929. Organization for physiological homeostasis. Physiol Rev 9, 399–431.
Cardoso, J.C.R., Laiz-Carrion, R., Louro, B., Silva, N., Canario, A.V.M., Mancera, J.M., Power, D.M., 2011. Divergence of duplicate POMC genes in gilthead sea bream Sparus auratus. Gen Comp Endocrinol 173, 396–404. https://doi.org/10.1016/j.ygcen.2010.12.001
Chepurny, O.G., Holz, G.G., 2007. A novel cyclic adenosine monophosphate-responsive luciferase reporter incorporating a nonpalindromic cyclic adenosine monophosphate response element provides optimal performance for use in G protein-coupled receptor drug discovery efforts. J Biomol Screen 12, 740–746. https://doi.org/10.1177/1087057107301856
Close, D.A., Yun, S.-S., McCormick, S.D., Wildbill, A.J., Li, W., 2010. 11-Deoxycortisol is a corticosteroid hormone in the lamprey. Proc Natl Acad Sci U S A 107, 13942–13947. https://doi.org/10.1073/pnas.0914026107
Dautzenberg, F.M., Kilpatrick, G.J., Hauger, R.L., Moreau, J.L., 2001. Molecular biology

of the CRH receptors - In the mood. Peptides 22, 753–760. https://doi.org/10.1016/S0196-9781(01)00388-6

Davidson, S.M., Rybka, A.E., Townsend, P.A., 2009. The powerful cardioprotective effects of urocortin and the corticotropin releasing hormone (CRH) family. Biochem Pharmacol 77, 141–150. https://doi.org/10.1016/j.bcp.2008.08.033

De Smet, W., 1962. Considerations on the stannius corpuscles and the interrenal tissues of bony fishes, especially based on researches into Amia. Acta Zool.

Dores, R.M., Chapa, E., 2021. Hypothesis and Theory: Evaluating the Co-Evolution of the Melanocortin-2 Receptor and the Accessory Protein MRAP1. Front Endocrinol (Lausanne) 12, 1–10. https://doi.org/10.3389/fendo.2021.747843

Dores, R.M., Liang, L., Davis, P., Thomas, A.L., Petko, B., 2016. Melanocortin receptors: Evolution of ligand selectivity for melanocortin peptides. J Mol Endocrinol 56, T119–T133. https://doi.org/10.1530/JME-15-0292

Dores, R.M., Mckinley, G., Meyers, A., Martin, M., Shaughnessy, C.A., 2022. Structure/Function Studies on the Activation Motif of Two Non-Mammalian Mrap1 Orthologs: Observations on the Phylogeny of Mrap1, Including a Novel Characterization of an Mrap1 from the Chondrostean Fish, Polyodon spathula. Biomolecules 12, 1681.

Dores, R.M., Scuba-Gray, M., McNally, B., Davis, P., Takahashi, A., 2018. Evaluating the interactions between red stingray (Dasyatis akajei) melanocortin receptors and elephant shark (Callorhinchus milii) MRAP1 and MRAP2 following stimulation with either stingray ACTH(1-24) or stingray Des-Acetyl-αMSH: A pharmacological study i. Gen Comp Endocrinol 265, 133–140. https://doi.org/10.1016/j.ygcen.2018.02.018

Dores, R.M., Smith, T.R., Rubin, D.A., Danielson, P., Marra, L.E., Youson, J.H., 1997. Deciphering posttranslational processing events in the pituitary of a neopterygian fish: Cloning of a gar proopiomelanocortin cDNA. Gen Comp Endocrinol 107, 401–413. https://doi.org/10.1006/gcen.1997.6947

Hoglin, B.E., Miner, M., Dores, R.M., 2022. Pharmacological properties of whale shark (Rhincodon typus) melanocortin-2 receptor and melancortin-5 receptor: Interaction with MRAP1 and MRAP2. Gen Comp Endocrinol 315, 113915.

Idler, D.R., O'Halloran, M.J., 1970. Steroids of a chondrostean: identification of

634 interrenal tissue in the American Atlantic sturgeon, Acipenser oxyrhynchus Mitchill,
635 by histological and histochemical methods. J Endocrinol 48, 621–626.
636 https://doi.org/10.1677/joe.0.0480621
637 Idler, D.R., Sangalang, G.B., 1970. Steroids of a chondrostean: in-vitro steroidogenesis
638 in yellow bodies isolated from kidneys and along the posterior cardinal veins of the
639 American Atlantic sturgeon, Acipenser oxyrhynchus mitchill. J Endocrinol 48, 627–
640 637.
641 Kusakabe, M., Zuccarelli, M.D., Nakamura, I., Young, G., 2009. Steroidogenic acute
642 regulatory protein in white sturgeon (Acipenser transmontanus): cDNA cloning,
643 sites of expression and transcript abundance in corticosteroidogenic tissue after an
644 acute stressor. Gen Comp Endocrinol 162, 233–240.
645 https://doi.org/10.1016/j.ygcen.2009.02.007
646 Leder, E.H., Silverstein, J.T., 2006. The pro-opiomelanocortin genes in rainbow trout
647 (Oncorhynchus mykiss): Duplications, splice variants, and differential expression. J
648 Endocrinol 188, 355–363. https://doi.org/10.1677/joe.1.06283
649 Liang, L., Sebag, J.A., Eagelston, L., Serasinghe, M.N., Veo, K., Reinick, C., Angleson,
650 J., Hinkle, P.M., Dores, R.M., 2011. Functional expression of frog and rainbow trout
651 melanocortin 2 receptors using heterologous MRAP1s. Gen Comp Endocrinol 174,
652 5–14. https://doi.org/10.1016/j.ygcen.2011.07.005
653 Noon, L.A., Franklin, J.M., King, P.J., Goulding, N.J., Hunyady, L., Clark, A.J.L., 2002.
654 Failed export of the adrenocorticotrophin receptor from the endoplasmic reticulum
655 in non-adrenal cells: evidence in support of a requirement for a specific adrenal
656 accessor. J Endocrinol 174, 17–25.
657 Okuta, A., Ando, H., Ueda, H., Urano, A., 1996. Two types of cDNAs encoding
658 proopiomelanocortin of Sockeye salmon, Oncorhynchus nerka. Zool Sci 13, 421–
659 427.
660 Pfaffl, M.W., 2001. A new mathematical model for relative quantification in real-time
661 RT–PCR. Nucleic Acids Res 29, 2003–2007. https://doi.org/10.1016/S0043-
662 1354(98)00516-8
663 Qi, J., Tang, N., Wu, Y., Chen, H., Wang, S., Wang, B., Xu, S., Wang, M., Zhang, X.,
664 Chen, D., Zhou, B., Li, Z., 2019. The transcripts of CRF and CRF receptors under

665 fasting stress in Dabry's sturgeon (Acipenser dabryanus Dumeril). Gen Comp
666 Endocrinol 280, 200–208. https://doi.org/10.1016/j.ygcen.2019.05.005
667 Reinick, C.L., Liang, L., Angleson, J.K., Dores, R.M., 2012. Identification of an MRAP-
668 independent melanocortin-2 receptor: Functional expression of the cartilaginous
669 fish, Callorhinchus milii, melanocortin-2 receptor in CHO cells. Endocrinology 153,
670 4757–4765. https://doi.org/10.1210/en.2012-1482
671 Schiöth, H.B., Haitina, T., Ling, M.K., Ringholm, A., Fredriksson, R., Cerdá-Reverter,
672 J.M., Klovins, J., 2005. Evolutionary conservation of the structural,
673 pharmacological, and genomic characteristics of the melanocortin receptor
674 subtypes. Peptides 26, 1886–1900. https://doi.org/10.1016/j.peptides.2004.11.034
675 Sebag, J.A., Hinkle, P.M., 2007. Melanocortin-2 receptor accessory protein MRAP
676 forms antiparallel homodimers. Proc Natl Acad Sci U S A 104, 20244–20249.
677 https://doi.org/10.1073/pnas.0708916105
678 Shaughnessy, C.A., Jensen, M.F., Dores, R.M., 2022. A basal actinopterygian
679 melanocortin receptor: Molecular and functional characterization of an Mc2r
680 ortholog from the Senegal bichir (Polypterus senegalus). Gen Comp Endocrinol
681 328, 114105.
682 Shaughnessy, C.A., McCormick, S.D., 2021. 11-Deoxycortisol is a stress responsive
683 and gluconeogenic hormone in a jawless vertebrate, the sea lamprey (Petromyzon
684 marinus). J Exp Biol 224, jeb241943. https://doi.org/10.1242/jeb.241943
685 Takahashi, A., Davis, P., Reinick, C., Mizusawa, K., Sakamoto, T., Dores, R.M., 2016.
686 Characterization of melanocortin receptors from stingray Dasyatis akajei, a
687 cartilaginous fish. Gen Comp Endocrinol 232, 115–124.
688 https://doi.org/10.1016/j.ygcen.2016.03.030
689 Valen, R., Jordal, A.E.O., Murashita, K., Rønnestad, I., 2011. Postprandial effects on
690 appetite-related neuropeptide expression in the brain of Atlantic salmon, Salmo
691 salar. Gen Comp Endocrinol 171, 359–366.
692 https://doi.org/10.1016/j.ygcen.2011.02.027
693 Wendelaar Bonga, S.E., 1997. The stress response in fish. Physiol Rev 77, 591–625.
694 https://doi.org/10.1152/physrev.1997.77.3.591
695 Williams, T.A., Bergstrome, J.C., Scott, J., Bernier, N.J., 2017. CRF and urocortin 3

protect the heart from hypoxia/reoxygenation-induced apoptosis in zebrafish. Am J Physiol - Regul Integr Comp Physiol 313, R91–R100. https://doi.org/10.1152/ajpregu.00045.2017

Winberg, S., Lepage, O., 1998. Elevation of brain 5-HT activity, POMC expression, and plasma cortisol in socially subordinate rainbow trout. Am J Physiol - Regul Integr Comp Physiol 274, 645–654. https://doi.org/10.1152/ajpregu.1998.274.3.r645

Wolverton, E.A., Wong, M.K.S., Davis, P.E., Hoglin, B., Braasch, I., Dores, R.M., 2019. Analyzing the signaling properties of gar (Lepisosteus oculatus) melanocortin receptors: Evaluating interactions with MRAP1 and MRAP2. Gen Comp Endocrinol 282, 113215. https://doi.org/10.1016/j.ygcen.2019.113215

Wong, M.K., Dores, R.M., 2022. Analyzing the Hypothalamus/Pituitary/Interrenal axis of the neopterygian fish, Lepisosteus oculatus: Co-localization of MC2R, MC5R, MRAP1, and MRAP2 in interrenal cells. Gen Comp Endocrinol 323–324, 114043. https://doi.org/10.1016/j.ygcen.2022.114043

Wunderink, Y.S., de Vrieze, E., Metz, J.R., Halm, S., Martínez-Rodríguez, G., Flik, G., Klaren, P.H.M., Mancera, J.M., 2012. Subfunctionalization of pomc paralogues in senegalese sole (solea senegalensis). Gen Comp Endocrinol 175, 407–415. https://doi.org/10.1016/j.ygcen.2011.11.026

Youson, J.H., Butler, D.G., 1985. Distribution and Structure of the Adrenocortical Homolog in Polypterus palmas Ayres. Acta Zool 66, 131–143. https://doi.org/10.1111/j.1463-6395.1988.tb00904.x

Youson, J.H., Butler, D.G., 1976. The andrenocortical homolog in the lake sturgeon, Acipenser fulvescens rafinesque. Am J Anat 145, 207–223. https://doi.org/10.1002/aja.1001450205

Youson, J.H., Butler, D.G., Bawks, B.A., 1988. Distribution and Structure of the Adrenocortical Homolog in the Reed-Fish (Calamoichthys calabaricus Smith). Acta Zool 69, 77–86. https://doi.org/10.1111/j.1463-6395.1988.tb00904.x

Figure 1: Sequence alignment and phylogenetic comparisons of sturgeon Mc2r and Mrap1. (A) Alignment of Atlantic (ao) and sterlet (ar) sturgeon Mc2rs with human (hs) MC2R. The 7 transmembrane (TM) domains are labeled. (B) Molecular phylogeny of sturgeon Mc2rs among gnathostome Mc2rs. The clade of Chondrichthyes was rooted as an outgroup. (C) Alignment of Atlantic sturgeon (ao) Mrap1 with Mrap1s from a selection of jawed vertebrates: human (hs), chicken (ch), bowfin (bf), and whale shark (ws). The activation motif (AM), reverse topology motif (RTM), and the membrane trafficking motif (MTM) are labeled. (D) Molecular phylogeny of aoMrap1 among gnathostome Mraps. In Panels A and C, shading indicates identical (dark) and similar (light) residues. In Panels B and D, numbers indicate bootstrap values (1000 replicates). See Materials and Methods for details of analyses and sequence accession numbers.

Figure 2: Pharmacology of sturgeon Mc2r co-expressed with vertebrate Mrap1s. Pharmacology of Mc2r of two sturgeons are described: (A,C) Atlantic sturgeon and (B, D) sterlet sturgeon. (A-B) Dose-response stimulation by human (h) ACTH(1-24) of sturgeon Mc2rs co-expressed without (Control) or with various vertebrate Mrap1s: bowfin (bf), chicken (ch), whale shark (ws). (C-D) Dose-response stimulation by either ACTH or α-MSH of sturgeon Mc2rs co-expressed with bfMrap1. Data are presented as mean ± standard error (n = 3) and lines represent fitted dose-response curve (three-parameter polynomial).

Figure 3: Pharmacology of sturgeon Mc2r co-expressed with sturgeon Mrap1. (A) Dose-response stimulation by human (h) ACTH(1-24) of Atlantic sturgeon (ao) Mc2r co-expressed without an Mrap (Control) or with either aoMrap1 or Mrap2. (B-C) Dose-response stimulation by hACTH(1-24) or α-MSH of Atlantic sturgeon Mc2r (B) and sterlet sturgeon (C) co-expressed without (Control) or with aoMrap1. Data are presented as mean ± standard error (n = 3) and lines represent fitted dose-response curve (three-parameter polynomial).

Figure 4: Transcription profiles of HPI axis genes in Atlantic sturgeon. Tissue profiles of an *a priori* selection of genes classically understood to be involved in an HPI

axis are presented as PCR products (A) and quantitative relative gene expression (B-G). Relative mRNA expression is presented as $2^{-\Delta CT}$ using several reference genes (*actb*, *gapdh*, and *ef1a*). Data are presented as mean ± standard error. See text for gene names/abbreviations.

Figure 5: Absence of yellow corpuscles and head kidney expression of *star* in Atlantic sturgeon. (A-B) Representative images of a dissection of Atlantic sturgeon body cavity with some internal organs in place (A) and removed (B) demonstrating the absence of yellow corpuscles along the dorsal body wall. For comparison, see white sturgeon dissection images presented by Kusakabe et al. (2009). (C-E) Tissue profile of *star* and *cyp11a1* are presented as PCR products (C) and relative mRNA expression ($2^{-\Delta CT}$) using several reference genes (*actb*, *gapdh*, and *ef1a*) (D-E). Data are presented as mean ± standard error.

FIGURE 1

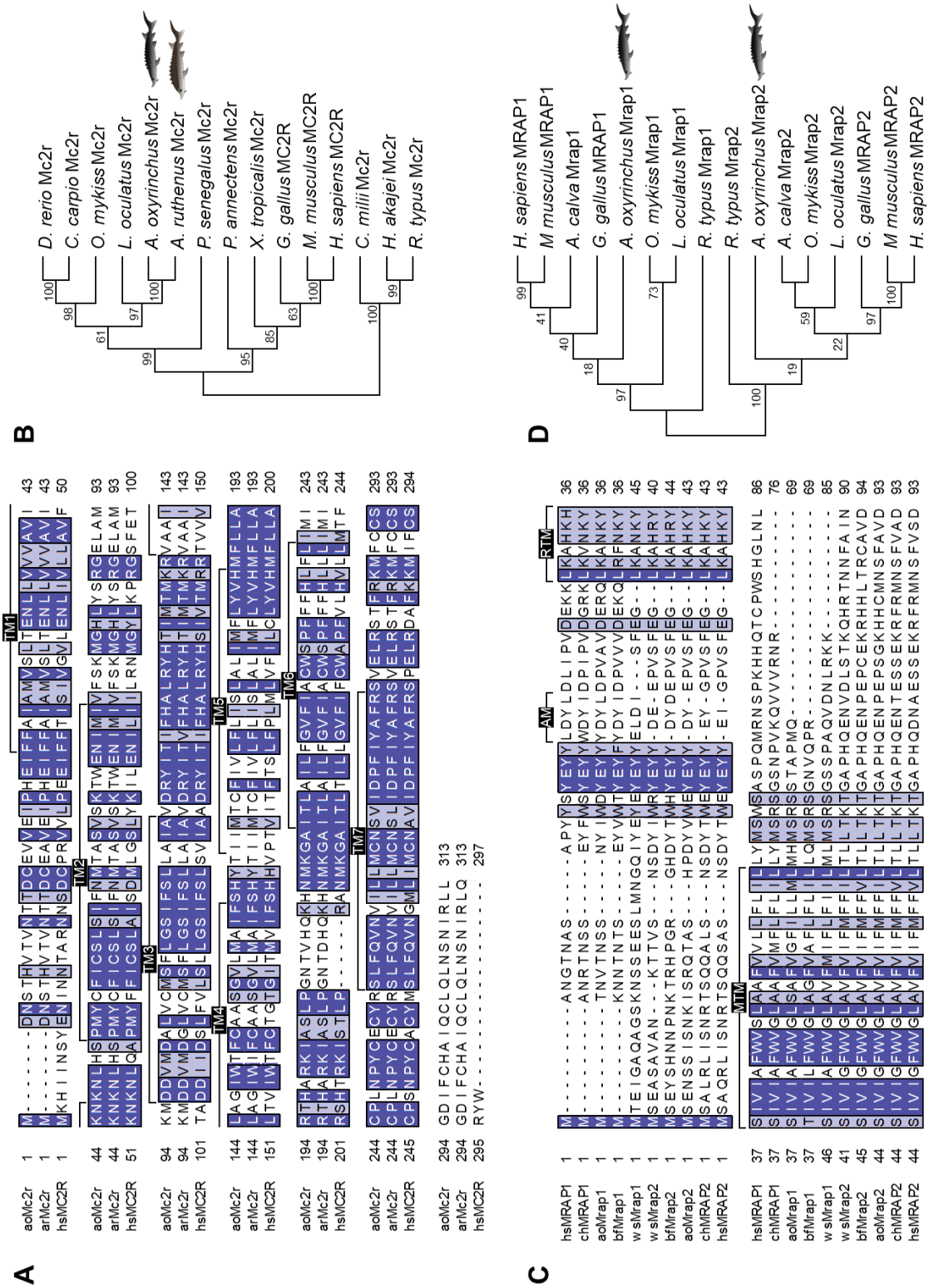
A
B
C
D
D. rerio Mc2r
C. carpio Mc2r
O. mykiss Mc2r
L. oculatus Mc2r
A. oxyrinchus Mc2r
A. ruthenus Mc2r
P. senegalus Mc2r
P. annectens Mc2r
X. tropicalis Mc2r
G. gallus MC2R
M. musculus MC2R
H. sapiens MC2R
C. milii Mc2r
H. akajei Mc2r
R. typus Mc2r
H. sapiens MRAP1
M musculus MRAP1
A. calva Mrap1
G. gallus MRAP1
A. oxyrinchus Mrap1
O. mykiss Mrap1
L. oculatus Mrap1
R. typus Mrap1
R. typus Mrap2
A. oxyrinchus Mrap2
A. calva Mrap2
O. mykiss Mrap2
L. oculatus Mrap2
G. gallus MRAP2
M musculus MRAP2
H. sapiens MRAP2

FIGURE 2

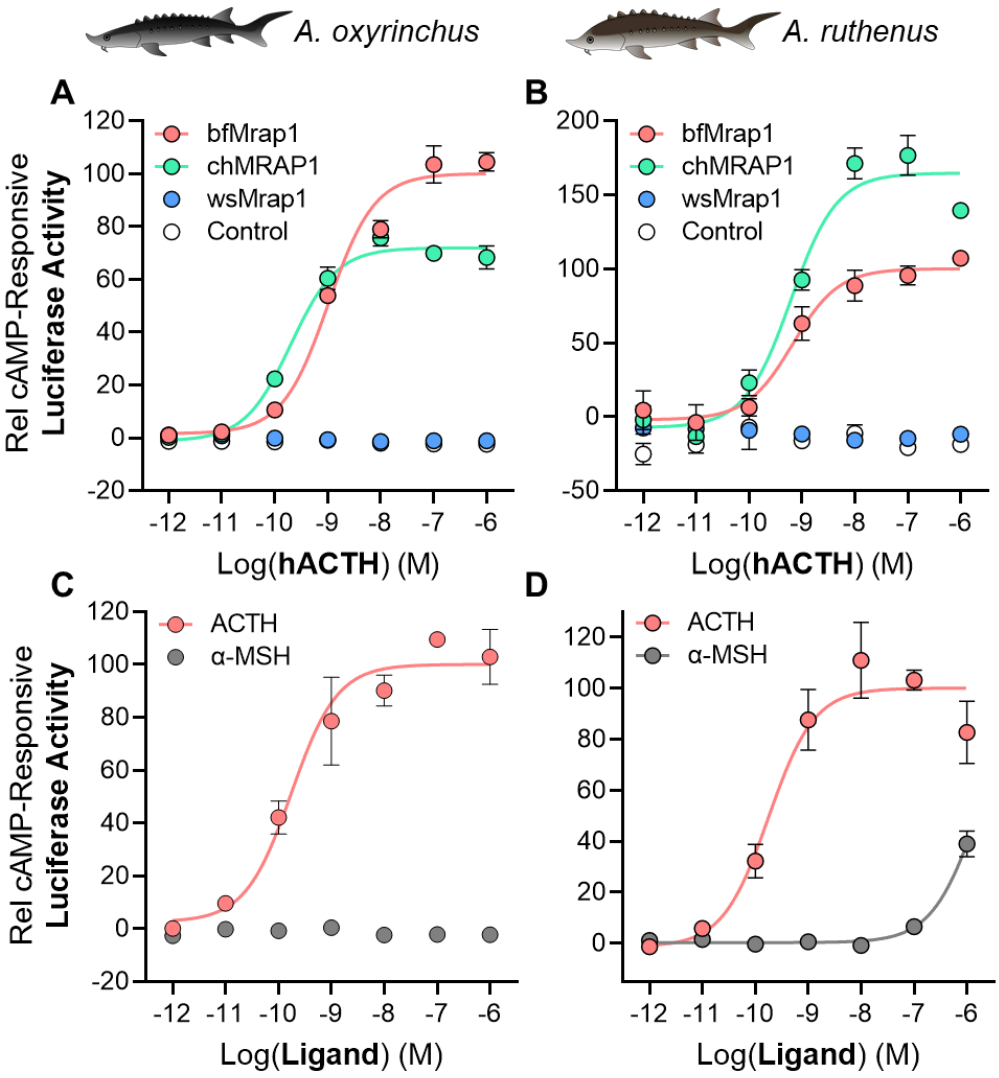
A. oxyrinchus
A. ruthenus
A
B
C
D
bfMrap1
chMRAP1
wsMrap1
Control
ACTH
α-MSH
Rel cAMP-Responsive Luciferase Activity
Log(hACTH) (M)
Log(Ligand) (M)

779

FIGURE 3

780

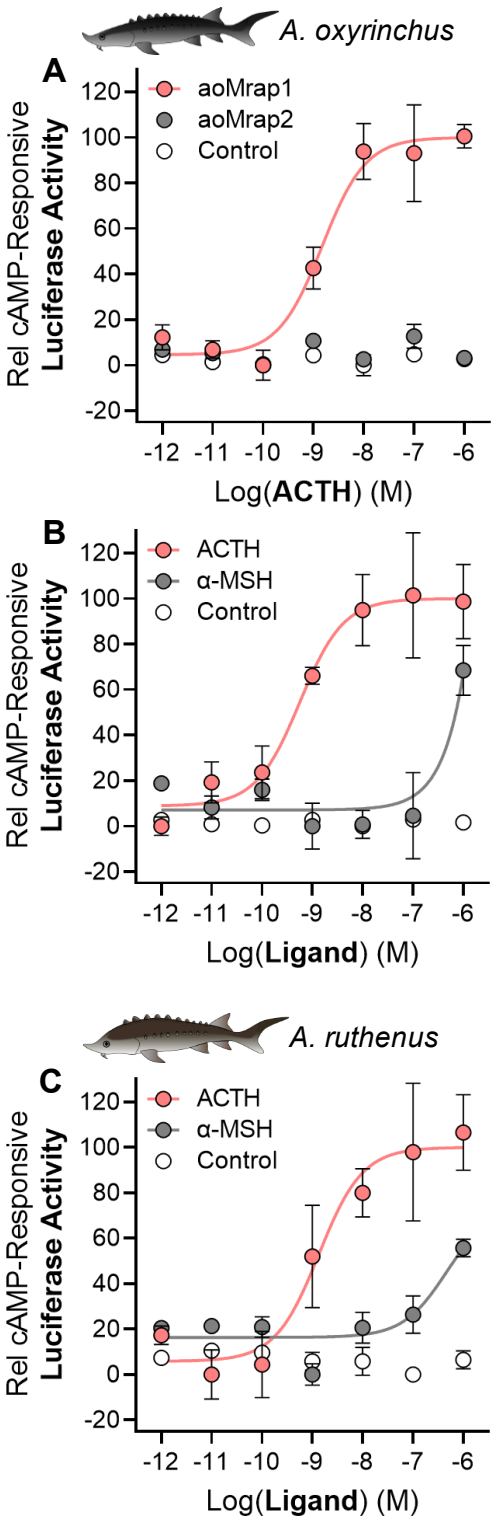

781

782

FIGURE 4

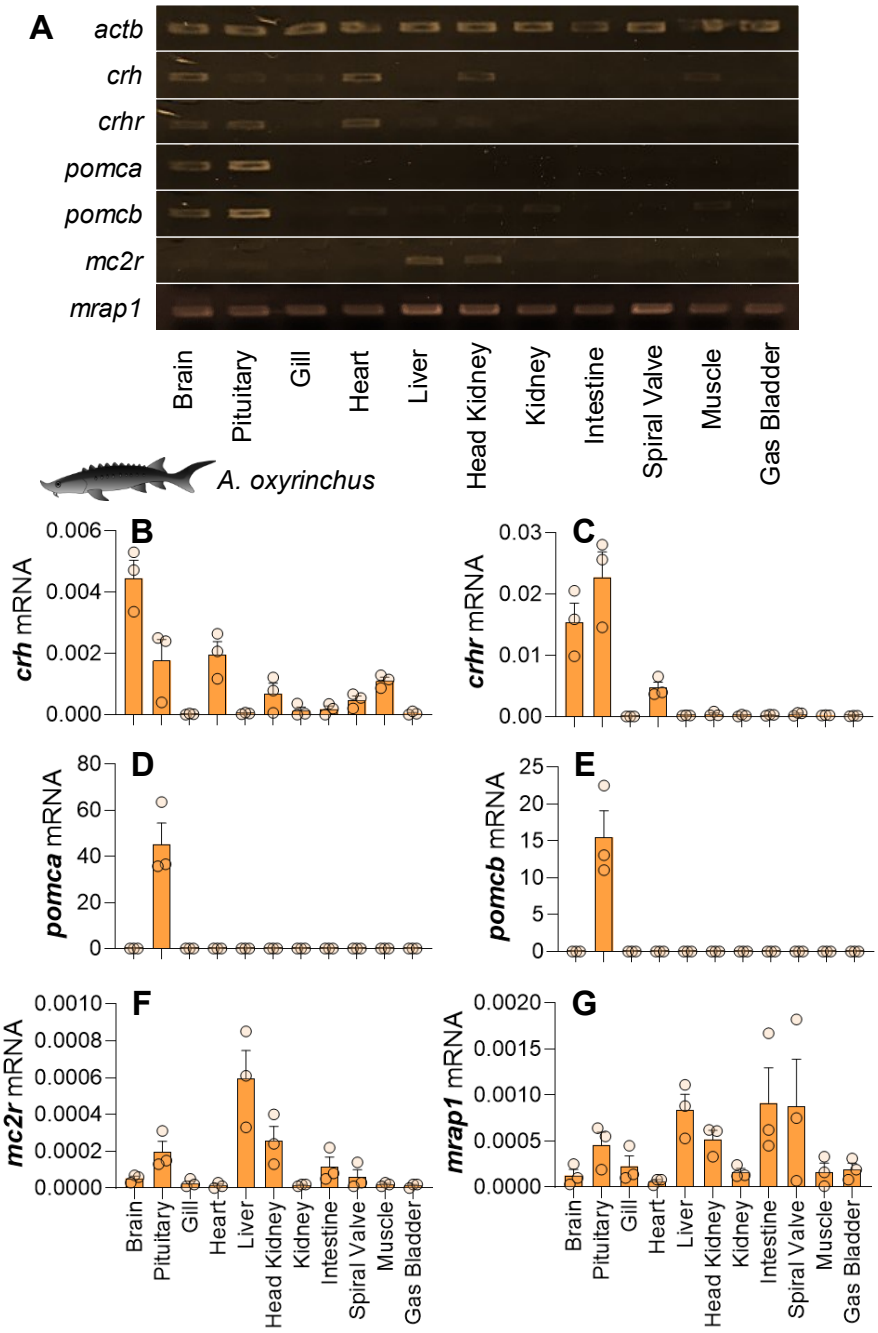
A
actb
crh
crhr
pomca
pomcb
mc2r
mrap1
Brain
Pituitary
Gill
Heart
Liver
Head Kidney
Kidney
Intestine
Spiral Valve
Muscle
Gas Bladder
A. oxyrinchus
B
crh mRNA
0.006
0.004
0.002
0.000
C
crhr mRNA
0.03
0.02
0.01
0.00
D
pomca mRNA
80
60
40
20
0
E
pomcb mRNA
25
20
15
10
5
0
F
mc2r mRNA
0.0010
0.0008
0.0006
0.0004
0.0002
0.0000
G
mrap1 mRNA
0.0020
0.0015
0.0010
0.0005
0.0000

787 **FIGURE 5**

788

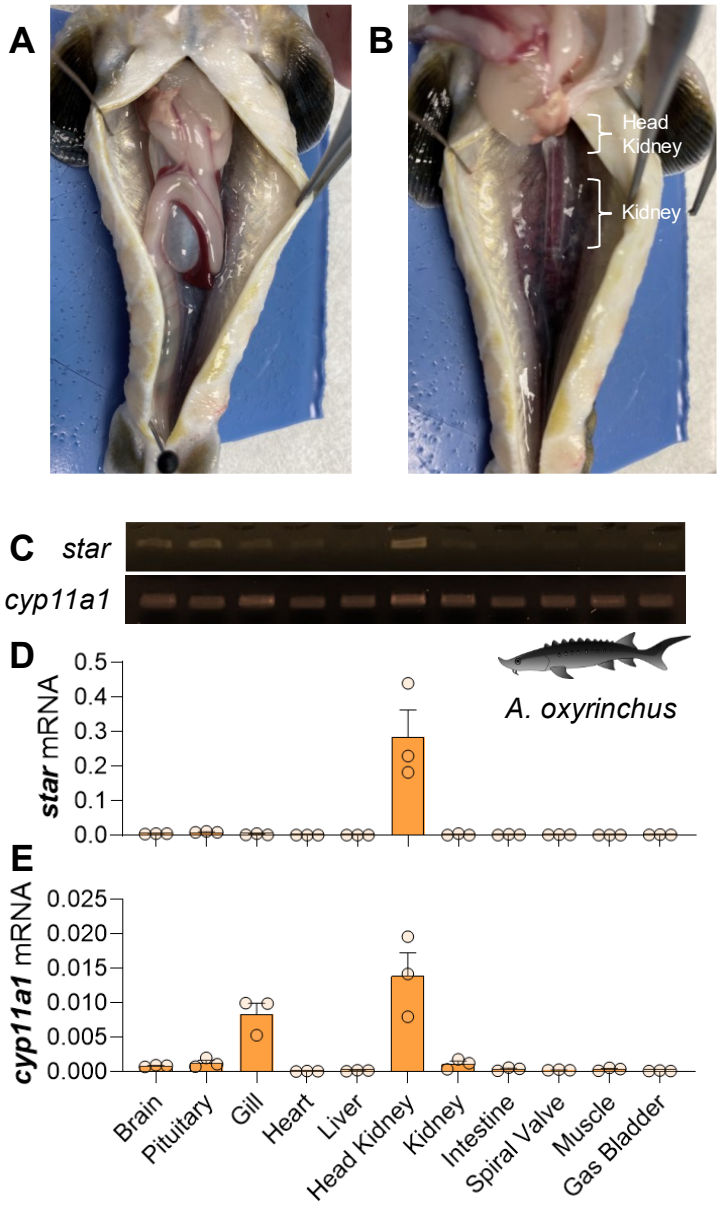

789

790

Table I: Atlantic sturgeon (*Acipenser oxyrinchus*) genes and PCR primers

Gene	Accession No.	Probe	Primer Sequence (5' – 3')	T_m (°C)	Length	Eff. (%)
actb	JABEPO010142615	F	ACCGCTGCTTCTTCTTCCTC	57.3	119	99
		R	CCCAAGAAGGATGGCTGGAA	57.3		
gapdh	JABEPO010032657	F	GTCAGCAATGCCTCTTGCAC	57.1	268	105
		R	GCTGTGTAGGCATGGACTGT	57.4		
ef1a	JABEPO010475780	F	GGGCAAGGGCTCCTTTAAGT	57.5	197	100
		R	TGCAAGTTATTACACATACCTGGG	54.9		
crh	JABEPO011127414	F	GCCTGACCCTCTGTCACATC	57.6	207	106
		R	ATGCTGCCAACTTTGCCTTG	56.9		
crhr	JABEPO011232047	F	GGAAAGCAGTGAAGGCCACT	57.9	84	105
		R	CATCGTCCCCTGGATTCACA	56.9		
pomca	JABEPO010530889	F	TGAAGCTTTATCCCAACCCAGAGAC	58.6	160	101
		R	GGGTACACCTTCACCGGAC	57.7		
pomcb	JABEPO010088828	F	AGCAGCGTTATCCCGACCCACAGAT	63.9	159	108
		R	GGGTACACCTTCACCGGAC	57.7		
mc2r	JABEPO010832850	F	TGGATGACGTAATGGACGCT	56.2	142	110
		R	GCAGCCACACGTTTCATTGT	56.7		
mrap1	JABEPO010347572	F	CTATTTGGATCCCGTTGCCG	56.2	83	115
		R	AAAGGCAGACAGACCAACCC	57.6		
star	JABEPO010801505	F	AGTAAGGTGCTCCCGGACAT	58.2	119	103
		R	GGGTTCCAGTCTCCCATCTG	57.2		
cyp11a1	JABEPO010537943	F	GGAGAGGATTGGCGATCCAG	57.5	161	88
		R	TGCCGTCCATCTTCCTTTCC	57.4		

T_m, annealing temperature (°C); Eff., real-time PCR reaction efficiency. Accession No. refers to *Acipenser oxyrinchus* genome assembly on NCBI (ASM1318447v1).

791

792

793

Table II: Curve fitting analyses for sturgeon Mc2r pharmacological experiments presented in Fig. 2 and Fig. 3.

Panel	Transfection	Ligand	Log(EC_{50}) (M)	V_{max} (%)
2A	aoMc2r	ACTH	–	–
	aoMc2r + wsMrap1	ACTH	–	–
	aoMc2r + chMRAP1	ACTH	-9.7 (-9.86, -9.52)	72 (68, 75)
	aoMc2r + bfMrap1	ACTH	-8.99 (-9.19, -8.77)	100 (94, 106)
2B	arMc2r	ACTH	–	–
	arMc2r + wsMrap1	ACTH	–	–
	arMc2r + chMRAP1	ACTH	-9.21 (-9.51, -8.94)	165 (150, 179)
	arMc2r + bfMrap1	ACTH	-9.18 (-9.55, -8.81)	100 (88, 112)
2C	aoMc2r + bfMrap1	ACTH	-9.76 (-10.15, -9.30)	100 (90, 110)
	aoMc2r + bfMrap1	α-MSH	–	–
2D	arMc2r + bfMrap1	ACTH	-9.75 (-10.13, -9.35)	100 (89, 111)
	arMc2r + bfMrap1	α-MSH	–	–
3A	aoMc2r	ACTH	–	–
	aoMc2r + aoMrap1	ACTH	-8.82 (-9.23, -8.40)	100 (86, 114)
	aoMc2r + aoMrap2	ACTH	–	–
3B	aoMc2r	ACTH	–	–
	aoMc2r + aoMrap1	ACTH	-9.25 (-9.95, -8.60)	100 (83, 118)
	aoMc2r + aoMrap1	α-MSH	–	–
3C	arMc2r	ACTH	–	–
	arMc2r + aoMrap1	ACTH	-8.87 (-9.61, -7.96)	100 (78, 125)
	arMc2r + aoMrap1	α-MSH	–	–

See text for definitions of abbreviations. Data are presented as mean ± 95% confidence intervals (indicated in parentheses; low, high).

794